# Articles

Contribution from the Department of Chemistry,
Iowa State University, Ames, Iowa 50011

## New Layered Phases Achieved with Centered Zirconium Chloride Clusters. The Stoichiometry $Zr_6Cl_{16}$

Robin P. Ziebarth and John D. Corbett*

*Received August 8, 1988*

The phase $Na_4Zr_6Cl_{16}Be$ is obtained in quantitative yield from the reaction of Zr powder, $ZrCl_4$, NaCl, and Be flakes in a sealed Ta container at 800 °C. A different, isostructural group of phases $Cs_3Zr_6Cl_{16}C$, $Cs_3Zr_6Cl_{16}B$, and $Cs_4Zr_6Cl_{16}Be$ were similarly obtained in ~90% yield from analogous reactions with CsCl, graphite, amorphous boron, etc.; reasonable yields of the first two occurred only when somewhat overreduced conditions were employed. The two structure types were established by single-crystal X-ray diffraction means for the following refined compositions: $Na_{3.9(1)}Zr_6Cl_{16}Be$, space group *Pcmm*, $Z = 4$, $a = 13.251$ (1) Å, $b = 14.319$ (1) Å, $c = 14.092$ (2) Å, $R = 4.3\%$, $R_w = 3.8\%$; $Cs_{3.04(3)}Zr_6Cl_{16}C$, space group $P2_1/n$, $Z = 4$, $a = 11.032$ (2) Å, $b = 11.851$ (3) Å, $c = 12.473$ (3) Å, $\beta = 108.01$ (2)°, $R = 6.2\%$, $R_w = 6.8\%$. Both structures contain puckered layers formed from $Zr_6Cl_{12}$-type clusters with $Cl^{a-a}$ atoms bridging four vertices into sheets plus two terminal $Cl^a$ occupying single trans positions, viz., $^2_\infty[Zr_6Cl_{12}Z]Cl^{a-a}{}_{4/2}Cl^a{}_2$, where the interstitial Z = Be, B, or C occupies all cluster centers. The cluster layers are separated and puckered to different degrees in order to provide suitable chlorine polyhedra between them to accommodate the cations. The latter fractionally occupy irregular sites that are minimally six- ($Na^+$) or seven-coordinate ($Cs^+$). The 15-electron cluster in the cesium salt exhibits shorter Zr–Zr and Zr–Zr distances than analogous 14-electron examples.

### Introduction

A variety of $M_6X_{12}$-type halide cluster compounds have been prepared over the past 20 years with $M_6X_{12}$ to $M_6X_{15}$ stoichiometries (M = Nb, Ta, Zr).[1-6] Other than those with the unusual $KZr_6Cl_{13}Be$ structure,[6,7] all of these cluster compounds are built upon various combinations of $M_6X^i{}_{12}$ units with bifunctional outer ($X^a$) halides bonded between all vertices of the clusters. Near the lower $M_6X_{12}$ limit, this requires cooperative $X^a$–$X^i$ linkages utilizing edge-bridging $X^i$ atoms in other clusters, while the composition $M_6X_{15}$ ($=M_6X^i{}_{12}X_{6/2}$) has only $X^{a-a}$ intercluster connectivities.

Extension of the series to larger X:M ratios by incorporation of a pair of unshared terminal $X^a$ atoms in place of one or more $X^{a-a}$ intercluster linkages has been realized only for the limiting $[M_6X^i{}_{12}]X^a{}_6$ case, where a number of niobium chloride and bromide clusters have been obtained.[2,8,9] The intermediate compositions $[M_6X_{12}]X_4$ and $[M_6X_{12}]X_5$ with appropriate combinations of $X^{a-a}$ intercluster connectivity and terminal $X^a$ atoms have not been previously observed. On the other hand, analogous compounds based on the $M_6X_8$-type of cluster, namely $[M_6X_8]X_4$ and $[M_6X_8]X_5$, have been synthesized. For instance, $[Mo_6X_8]X_4$ phases with X = Cl, Br, and I[10] have been known since the late 1960s, and more recently, a variety of molybdenum and rhenium phases with $M_6X_8$-type clusters have been prepared with the $[M_6X_8]X_4$ and $[M_6X_8]X_5$ stoichiometries.[11,12]

The apparent stability of $Zr_6Cl_{12}Z$ clusters with 14 cluster-bonding electrons, the relative ease with which different second-period elements Z may be incorporated into the $Zr_6Cl_{12}$ cluster, and the opportunities to add additional $M^I$ cations within the cluster framework structure[6,7,13-15] suggested that compounds within the $Zr_6X_{15}$ to $Zr_6X_{18}$ sequence might be prepared by appropriate choices of interstitial atoms in concert with the number of cations. Although the oxide $Zr_6Cl_{16}O$ would be an obvious 14-electron target, the stability of $ZrClO_x$ ($0 \le x \le 0.43$)[16] even under moderately oxidizing conditions appears to preclude the formation of oxygen-centered clusters with zirconium. As is often the case in synthetic chemistry, the first $[Zr_6Cl_{12}]Cl_4$-type compound, $Na_4Zr_6Cl_{16}Be$, was prepared by accident. The second, $Cs_3Zr_6Cl_{16}C$, was synthesized more by design, while the isostructural $Cs_3Zr_6Cl_{16}B$ and $Cs_4Zr_6Cl_{16}Be$ were prepared as planned. Other members of the series that exhibit a $Zr_6X_{17}Z$ composition have not yet been recognized.

### Experimental Section

The materials utilized, the general synthetic techniques utilizing sealed Ta containers, Guinier powder diffraction and cell parameter refinement methods, otherwise uncited crystallographic programs for absorption correction and refinement (ALLS, FOUR), etc., and the sources of the scattering factors (which included real and imaginary components of anomalous dispersion) were as referenced or described before.[14,17]

**Syntheses.** The $Na_4Zr_6Cl_{16}Be$ phase was initially synthesized in a reaction designed to yield the composition $Na_3Zr_6Cl_{15}Be$. The recently completed crystal structure of $Na_{0.5}Zr_6Cl_{15}C$[18] had established that the sodium cations partially occupied a 48-fold site in the chlorine lattice. Complete occupation of the site, which would require three cations per cluster, coupled with an interstitial atom that would yield 14 cluster-bonding electrons, suggested that $Na_3Zr_6Cl_{15}Be$ might be prepared in the $Ta_6Cl_{15}$ structure[3] or a distorted version thereof such as $Na_2Zr_6Cl_{15}B$.[18] The initial reaction, which was loaded with stoichiometric amounts of Zr powder, $ZrCl_4$, NaCl, and Be flakes plus a 40% excess of NaCl, produced

(1) Schäfer, H.; Schnering, H.-G. *Angew Chem.* **1964**, *76*, 833.
(2) Wells, A. F. *Structural Inorganic Chemistry*, 5th ed.; Clarendon Press: Oxford, England, 1984; pp 432-437.
(3) Bauer, D.; von Schnering, H.-G. *Z. Anorg. Allg. Chem.* **1968**, *361*, 259.
(4) Simon, A.; von Schnering, H.-G.; Wöhrle, H.; Schäfer, H. *Z. Anorg. Allg. Chem.* **1965**, *339*, 155.
(5) Corbett, J. D.; Daake, R. L.; Poeppelmeier, K. R.; Guthrie, D. H. *J. Am. Chem. Soc.* **1978**, *100*, 652.
(6) Ziebarth, R. P.; Corbett, J. D. *J. Am. Chem. Soc.* **1985**, *107*, 4571.
(7) Ziebarth, R. P.; Corbett, J. D. To be submitted for publication.
(8) Simon, A.; von Schnering, H.-G.; Schäfer, H. *Z. Anorg. Allg. Chem.* **1968**, *361*, 235.
(9) Ueno, F.; Simon, A. *Acta Crystallogr., Sect. C* **1985**, *41*, 308.
(10) Schäfer, H.; von Schnering, H.-G.; Tillack, J.; Kuhnen, F.; Wöhrle, H.; Baumann, H. *Z. Anorg. Allg. Chem.* **1967**, *353*, 281.
(11) Leduc, L.; Perrin, A.; Sergent, M. *C. R. Seances Acad. Sci., Ser. 2* **1983**, *296*, 961.
(12) Perrin, C.; Sergent, M. *J. Less-Common Met.* **1986**, *123*, 117.
(13) Smith, J. D.; Corbett, J. D. *J. Am. Chem. Soc.* **1985**, *107*, 5704.
(14) Ziebarth, R. P.; Corbett, J. D. *J. Am. Chem. Soc.* **1987**, *109*, 4844.
(15) Ziebarth, R. P.; Corbett, J. D. *J. Am. Chem. Soc.* **1988**, *110*, 1132.
(16) Seaverson, L. M.; Corbett, J. D. *Inorg. Chem.* **1983**, *22*, 2789.
(17) Hwu, S.-J.; Corbett, J. D.; Poeppelmeier, K. R. *J. Solid State Chem.* **1985**, *57*, 43.
(18) Ziebarth, R. P.; Corbett, J. D. *J. Less-Common Met.* **1988**, *137*, 21.

0020-1669/89/1328-0626$01.50/0 

instead a nearly quantitative yield of the new compound $Na_4Zr_6Cl_{16}Be$ after 2 weeks at 800 °C. (The composition employed corresponded to the stoichiometry $Na_{4.2}Zr_6Cl_{16.2}Be$.) Reactions loaded for the composition $Na_4Zr_6Cl_{16}Be$ produce dark red, rectangular parallelepipeds of the desired compound at 800 °C in 95+% yield. (The yield criterion means that the product was single phase to Guinier powder diffraction according to a careful comparison of the pattern with that calculated for the structure subsequently determined.) The original compound sought, $Na_3Zr_6Cl_{15}Be$, has not yet been obtained. Reactions utilizing stoichiometric proportions of Zr powder, $ZrCl_4$, NaCl, and Be yield a mixture of $Zr_6Cl_{12}Be$[7] and $Na_4Zr_6Cl_{16}Be$ at 800–850 °C.

On the basis of the powder diffraction data, a cation exchange between $Na_4Zr_6Cl_{16}Be$ and $KAlCl_4$(l) occurs at 300 °C. The reaction is believed to produce a $K_4Zr_6Cl_{16}Be$ phase in a different structure with more puckered cluster sheets than in $Na_4Zr_6Cl_{16}Be$, but the product has not been characterized further.

The new compound $Cs_3Zr_6Cl_{16}C$ was obtained as a dark brown, highly crystalline material in ~90% yield from an 850 °C reaction designed to synthesize $Cs_3Zr_6Cl_{15}C$ from stoichiometric quantities of Zr powder, $ZrCl_4$, CsCl, and graphite. The other more reduced product was not identified. This choice of reaction stoichiometry was prompted by similar reactions with other alkali-metal chlorides ($M^I$ = Na, K, Rb) that had yielded compounds of unknown composition and structure. Unfortunately, crystal intergrowth and twinning problems had prevented a structural study of these, and it was hoped that a larger cation might reduce the single crystal problems. The cesium-containing compound obtained, although not isostructural with the unknown products from the other $M^ICl$ reactions, was however new from a structural and compositional viewpoint.

The reducing conditions produced by the chlorine-poor reaction stoichiometry employed above appear to be important in preparing the 15-electron clusters in $Cs_3Zr_6Cl_{16}C$. A reaction with approximately 5% more $ZrCl_4$ produced a mixture of the 14-electron cluster phase $CsZr_6Cl_{15}C$[14] with $Cs_2ZrCl_6$. Small excesses (<5%) of CsCl and $ZrCl_4$ over the $Cs_3Zr_6Cl_{15}C$ stoichiometry produced an unidentified compound with a cell volume slightly less than twice that of $Cs_3Zr_6Cl_{16}C$ in more than 90% yield. Several nice single crystals were obtained, but the structure, which presumably contains eight cluster units per cell, has not been solved.[19]

It is important to note that the addition of the stoichiometric amount of carbon, beryllium, etc. is absolutely essential in order to obtain the indicated phases in high yield, providing compelling evidence for quantitative occurrence of the indicated interstitial that was refined in subsequent X-ray studies. Omission of just this minor reactant gave mixed, cluster-free products, primarily $M^I_2ZrCl_6$, $M^ICl$, and ZrCl.

Two additional compounds have also been prepared that are isostructural with $Cs_3Zr_6Cl_{16}C$ according to Guinier powder diffraction. The phase $Cs_3Zr_6Cl_{16}B$ was prepared in about 90% yield from an 850 °C reaction of amounts of Zr powder, $ZrCl_4$, CsCl and amorphous boron powder appropriate to the composition $Cs_3Zr_6Cl_{15}B$. As was observed for the carbide, more oxidizing reaction conditions yield a different compound which, in this case, is both unknown and different from the unknown carbide. The nominal composition $Cs_4Zr_6Cl_{16}Be$ in the same structure was obtained in about 90% yield from a reaction of the appropriate stoichiometry that was heated at 850 °C for 2 weeks. A small amount of $Cs_2ZrCl_6$ was also observed in the powder diffraction pattern of the product. The exact cesium contents of the boride and beryllide compounds are not known, but these are crystallographically limited to four cesium atoms per cluster. The preference for electronic configurations with 14 cluster-bonding electrons suggests the listed compositions of $Cs_3Zr_6Cl_{16}B$ and $Cs_4Zr_6Cl_{16}Be$. Additional work in these systems will be necessary to determine the actual compositions as well as the nature of the unknown compounds prepared.

**Crystallography.** Two octants of data were collected at room temperature to $2\theta = 55°$ on a small rectangular prism of $Na_4Zr_6Cl_{16}Be$ using monochromatic Mo K$\alpha$ radiation. The orthorhombic unit cell, chosen on the basis of a small set of reflections indexed with the program BLIND,[20] was verified by axial photographs taken on the diffractometer which showed the expected layer spacings and mirror symmetry. The minimal absorption effects were corrected for by using a $\psi$-scan method. Details of the data collection and refinement are given in Table I.

The space group *Pccn* was chosen for the compound on the basis of the observed systematic extinctions and was verified subsequently by the successful refinement of the structure in it. The structure was solved by direct methods using the program MULTAN-80.[21] Four randomly oriented, octahedral $Zr_6$ clusters were included as "molecular fragments" in the normalization routine. Three zirconium positions identified in this way were used to phase a subsequent Fourier map from which the majority of the chlorine atoms in the structure were identified. Successive cycles of least-squares refinement and Fourier map synthesis were used to locate the remaining atoms. The interstitial beryllium atom was observed as an approximately three-electron residual in the cluster center following isotropic refinement of the zirconium and chlorine atoms in the structure and was included thereafter. The data were reweighted in 10 overlapping groups sorted on $F_o$ in order to correct for underestimated errors in the weaker reflections. Finally, a secondary extinction correction was applied to give residuals at convergence of $R = 4.3\%$ and $R_w = 3.8\%$. The final difference map was flat to less than $\pm 0.5$ e/Å$^3$. The refined occupancies of Na(1), Na(2), Na(3), and Be were, respectively, 0.97 (2), 0.60 (2), 0.79 (2), and 1.06 (2). Taking into account the different multiplicities of the sodium sites, the refined composition is $Na_{3.9(1)}Zr_6Cl_{16}Be$. The sodium coefficient is subsequently rounded to 4 in other places in this article.

**Table I.** Selected Crystallographic Data for $Na_4Zr_6Cl_{16}Be$ and $Cs_3Zr_6Cl_{16}C$

| | $Na_4Zr_6Cl_{16}Be$ | $Cs_3Zr_6Cl_{16}C$ |
|---|---|---|
| space group | *Pccn* (No. 56) | $P2_1/n$ (No. 14) |
| $Z$ | 4 | 4 |
| $a$,[a] Å | 13.251 (1) | 11.032 (2) |
| $b$, Å | 14.319 (1) | 11.851 (3) |
| $c$, Å | 14.092 (2) | 12.473 (3) |
| $\beta$, deg | (90) | 108.01 (2) |
| $V$, Å$^3$ | 2674.0 (5) | 1550.8 (6) |
| $\mu$, cm$^{-1}$ (Mo K$\alpha$) | 39.6 | 67.4 |
| transmission coeff range | 0.89–1.00 | 0.74–1.00 |
| $R$,[b] % | 4.3 | 6.2 |
| $R_w$,[b] % | 3.8 | 6.8 |

[a] Lattice parameters from Guinier powder data with Si as an internal standard; $\lambda = 1.54056$ Å. [b] $R = \sum||F_o| - |F_c||/\sum|F_o|$; $R_w = [\sum w(|F_o| - |F_c|)^2/\sum w|F_o|^2]^{1/2}$; $w = 1/\sigma_F^2$.

Four octants of single-crystal diffraction data were collected at room temperature to $2\theta = 55°$ on a dark brown, rectangular prism of $Cs_3Zr_6Cl_{16}C$ by using monochromatic Mo K$\alpha$ radiation. A monoclinic cell was deduced from a set of low-angle reflections indexed by using BLIND.[20] Axial photographs taken on the diffractometer were consistent in terms of symmetry and axial lengths with the chosen monoclinic cell. Pertinent crystallographic data are compiled in Table I.

The systematic extinctions observed in the data set and an assumed centricity uniquely identified the space group as $P2_1/n$. The phase problem was again solved by direct methods using MULTAN-80 with two randomly oriented $Zr_6$ clusters included as "molecular fragments". The three most intense peaks in the Fourier synthesis calculated from the phase set were assigned to zirconium atoms and used as a starting point for subsequent calculations. The remaining atoms in the structure were located by successive cycles of least-squares refinement and Fourier map calculations. The carbon atom was found as a six-electron residual in the cluster center at (0, 0, 0) following isotropic refinement of the zirconium, chlorine, and cesium atoms and was added to the model at that point. Anisotropic refinement of all atoms but carbon followed by a reweighting of the data set (above) gave final residuals of $R = 6.2$ and $R_w = 6.8\%$. The Cs(1) and Cs(2) positions refined to occupancies of 0.983 (7) and 0.535 (6), respectively, for a total of 3.04 (3) cesium atoms per $Zr_6Cl_{16}Be$ cluster. The refinement converged with a carbon atom occupancy of 1.2 (1) with $B = 2.6$ (8) Å$^2$.

The final difference map was littered with a sizable number of ~±0.5-electron residuals. In addition, a peak of approximately three electrons was observed between cluster layers about midway between Cs(2) atoms along $b$. When included in the model as a fractional cesium atom, the residual refined to an occupancy of 0.126 (5), an isotropic $B$ of 6.3 (4), and fractional coordinates of (0.333 (1), 0.494 (1), –0.001 (1)). $R$ and $R_w$ naturally improved to 5.1 and 5.3%, respectively. The position was surrounded by five chlorine atoms at plausible distances of 3.40–3.55 Å, but it also had two cesium neighbors at unreasonably short distances, ~3.05 Å. Although the residual could be interpreted as a small amount of cation disorder between the cluster layers, with the residual site occupied by cesium only when the two nearest neighbor cation sites are

(19) Centered orthorhombic cell, space group = *Cmcm* or *Cmc2*; $a = 18.518$, $b = 31.022$, $c = 18.406$ Å.

(20) Jacobson, R. A. *J. Appl. Crystallogr.* **1976**, *9*, 115.

(21) Main, P.; Fiske, S. J.; Hull, S. E.; Lessinger, L.; Germain, G.; Declerq, J. P.; Woolfson, M. M. "MULTAN 80. A System of Computer Programs for the Automatic Solution of Crystal Structures from X-Ray Diffraction Data"; Department of Physics, University of York Printing Unit: York, England, 1980.

**Table II.** Positional Parameters for $Na_4Zr_6Cl_{16}Be$

| atom | x | y | z |
|---|---|---|---|
| Zr(1) | 0.97817 (8) | 0.40092 (6) | 0.37087 (6) |
| Zr(2) | 0.52704 (8) | 0.37501 (6) | 0.10262 (6) |
| Zr(3) | 0.17340 (7) | 0.46780 (6) | 0.50062 (8) |
| Cl(1) | 0.3420 (2) | 0.3299 (2) | 0.1153 (2) |
| Cl(2) | 0.7200 (2) | 0.3954 (2) | 0.1125 (2) |
| Cl(3) | 0.2873 (2) | 0.5743 (2) | 0.1433 (2) |
| Cl(4) | 0.6656 (2) | 0.6438 (2) | 0.1440 (2) |
| Cl(5) | 0.5081 (2) | 0.4725 (2) | 0.2569 (2) |
| Cl(6) | 0.8712 (2) | 0.5662 (2) | 0.0050 (2) |
| Cl(7) | 0.4481 (2) | 0.7236 (2) | 0.2769 (2) |
| Cl(8) | 0.4423 (2) | 0.7466 (2) | 0.0301 (2) |
| Na(1)[a] | 0.5520 (4) | 0.0890 (3) | 0.0830 (3) |
| Na(2)[b] | 0.6264 (7) | 0.8295 (6) | 0.1742 (6) |
| Na(3)[c] | 1/4 | 3/4 | 0.2248 (7) |
| Be[d] | 1/2 | 1/2 | 0 |

[a] Occupancy refined to 0.97 (2). [b] Occupancy refined to 0.60 (2). [c] Occupancy refined to 0.79 (2). [d] Occupancy refined to 1.06 (6).

**Table III.** Interatomic Distances in $Na_4Zr_6Cl_{16}Be$ (Å)

| | | | |
|---|---|---|---|
| | | Zr–Zr | |
| Zr(1)–Zr(2) (×2)[a] | 3.288 (1) | Zr(2)–Zr(3) (×2) | 3.299 (1) |
| Zr(1)–Zr(2) (×2) | 3.294 (1) | Zr(2)–Zr(3) (×2) | 3.308 (1) |
| Zr(1)–Zr(3) (×2) | 3.294 (1) | $\bar{d}$ | 3.299 |
| Zr(1)–Zr(3) (×2) | 3.310 (1) | | |
| | | Zr–Be | |
| Zr(1)–Be (×2) | 2.3255 (9) | Zr(3)–Be (×2) | 2.3436 (9) |
| Zr(2)–Be (×2) | 2.3286 (9) | $\bar{d}$ | 2.333 |
| | | Zr–$Cl^i$ | |
| Zr(1)–Cl(3) (×2) | 2.561 (3) | Zr(2)–Cl(5) (×2) | 2.596 (3) |
| Zr(1)–Cl(4) (×2) | 2.574 (3) | Zr(3)–Cl(1) (×2) | 2.559 (3) |
| Zr(1)–Cl(8) (×2) | 2.576 (3) | Zr(3)–Cl(3) (×2) | 2.576 (3) |
| Zr(1)–Cl(5) (×2) | 2.585 (3) | Zr(3)–Cl(4) (×2) | 2.592 (3) |
| Zr(2)–Cl(1) (×2) | 2.542 (3) | Zr(3)–Cl(2) (×2) | 2.600 (3) |
| Zr(2)–Cl(2) (×2) | 2.578 (3) | $\bar{d}$ | 2.577 |
| Zr(2)–Cl(8) (×2) | 2.588 (3) | | |
| | | Zr–$Cl^{a-a}$ | |
| Zr(1)–Cl(7) (×2) | 2.771 (3) | Zr(2)–Cl(7) (×2) | 2.773 (3) |
| | | Zr–$Cl^a$ | |
| Zr(3)–Cl(6) (×2) | 2.667 (3) | | |
| | | Na–Cl | |
| Na(1)–Cl(6) (×1) | 2.681 (5) | Na(2)–Cl(5) (×1) | 2.883 (9) |
| Na(1)–Cl(6) (×1) | 2.717 (6) | Na(2)–Cl(1) (×1) | 2.997 (9) |
| Na(1)–Cl(7) (×1) | 2.759 (5) | Na(2)–Cl(7) (×1) | 3.159 (9) |
| Na(1)–Cl(8) (×1) | 2.844 (5) | Na(2)–Cl(8) (×1) | 3.389 (9) |
| Na(1)–Cl(5) (×1) | 2.916 (5) | Na(2)–Zr(2) (×1) | 3.802 (9) |
| Na(1)–Cl(2) (×1) | 3.058 (6) | Na(2)–Zr(1) (×1) | 3.893 (8) |
| Na(1)–Na(1) (×1) | 3.724 (9) | Na(2)–Na(2) (×1) | 3.99 (2) |
| Na(1)–Zr(1) (×1) | 4.078 (4) | Na(3)–Cl(7) (×2) | 2.752 (4) |
| Na(2)–Cl(4) (×1) | 2.743 (9) | Na(3)–Cl(3) (×2) | 2.810 (5) |
| Na(2)–Cl(6) (×1) | 2.813 (9) | Na(3)–Cl(2) (×2) | 3.122 (8) |
| Na(2)–Cl(4) (×1) | 2.814 (9) | Na(3)–Zr(1) (×2) | 3.953 (3) |

[a] Number of times the distance occurs per cluster or cation.

unoccupied, this is presently not believed to be an inherent feature of the structure. It is more likely that the residual is associated with the poor quality and small size of the data crystal. This latter interpretation is supported by a second crystal structure determination of an isostructural $Cs_3Zr_6Cl_{16}Z$ phase.[22] The crystal used in the determination was of unknown origin as it has been accidentally picked up in the crystal mounting box. The identity of the interstitial atom was uncertain, but it was certainly limited to C or B. The structural refinement, which converged to $R = 5.2$ and $R_w = 4.8\%$ with a carbon atom in the cluster center, gave very similar atom positions and distances. More importantly, there was only a residual of less than 1 e/Å$^3$ at the former interlayer position of the three-electron residual. In light of the results of this second structural result, the three-electron residual was not included in the final stages of the present study. It should be noted that the higher $R$ values in this structure compared with those of other zirconium chloride cluster phases are largely associated with this ignored residual.

(22) Hughbanks, T.; Dudis, D. S.; Corbett, J. D. Unpublished research, 1986.

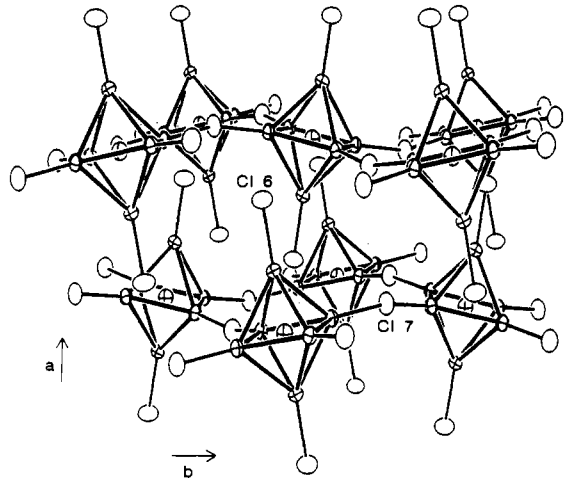


**Figure 1.** Approximately [001] view of the structure of $Na_4(Zr_6Cl^i_{12}Be)Cl_4$. All $Cl^i$ and Na atoms have been omitted for clarity. The 2-fold axes parallel to $\vec{c}$ in the tunnel-like structures between layers relate the top layer centered about $x = {}^1/_2$ to the bottom layer around $x = 0$ (90% probability thermal ellipsoids).

Final positional parameters for $Na_{4.0}Zr_6Cl_{16}Be$ and $Cs_3Zr_6Cl_{16}C$ are listed in Tables II and III, respectively. The thermal parameters of the atoms plus the observed and calculated structure factor amplitudes are available as supplementary material.

## Results and Discussion

The two new $Zr_6Cl_{16}Z$ structures $Na_4Zr_6Cl_{16}Be$ and $Cs_3Zr_6Cl_{16}C$ are built up of two-dimensional networks of interconnected $Zr_6Cl^i_{12}Z$ clusters like the analogous $(Mo_6X^i_8)X_4$ binary phases.[10] Four $Cl^{a-a}$ atoms bonded at zirconium vertices perpendicular to a pseudo-4-fold axis serve to link adjacent clusters into a puckered four-connected net, while unshared $Cl^a$ atoms fill the two remaining trans positions above and below this cluster sheet. The two-dimensional intercluster connectivity is symbolically formulated $^2_\infty[Zr_6Cl^i_{12}Z]Cl^{a-a}{}_{4/2}Cl^a_2$. However, significant differences exist between $Na_4Zr_6Cl_{16}Be$ and $Cs_3Zr_6Cl_{16}C$, particularly with respect to cell symmetries, cation sites, and, especially, relative cluster orientations and the puckering of the layers.

**$Na_4Zr_6Cl_{16}$.** The two-dimensional cluster sheets in $Na_4Zr_6Cl_{16}Be$ pack in a staggered fashion such that $Cl^a$ atoms from clusters in one layer lie in voids in the cluster layers above and below. The cluster layers stack in the $\vec{a}$ direction as is illustrated in Figure 1. The relative orientation of the cluster layers with respect to one another is generated by 2-fold axes situated between cluster layers at $y = {}^1/_4$ and ${}^3/_4$. The interlayer separation, $\vec{a}/2$, is 6.63 Å. The slightly puckered appearance of the layers results from an approximately ±11° canting of the clusters within each layer from the direction normal, primarily in the $\vec{b}$ direction. Every other row of clusters within the sheet is tilted in the opposite direction. Four sodium cations per cluster are distributed above, below, and within the cluster layers and electrostatically bind the anionic layers together. In $[Mo_6Cl^i_8]Cl_4$, the $M_6X^i_8$-type cluster structural analogue of $[Zr_6Cl^i_{12}]Cl_4$, the layers pack in a similar manner;[10] however, there are no cations present, and canting of the clusters within the layers is not observed.

The $Zr_6Cl^i_{12}Be$ cluster, the principal component of the layers, has crystallographically imposed $\bar{1}$ symmetry. Relevant interatomic distances are given in Table IV. The cluster is slightly elongated normal to the cluster sheet and toward $Cl^a$. The Zr–Zr distances within the layer average 3.291 Å, while those roughly perpendicular to the layer average 3.303 Å, presumably a reflection of stronger bonding between terminal zirconium and chlorine. The Zr–Be distances of 2.32–2.34 Å are consistent with the analogous distances in other beryllium-centered zirconium chloride clusters, e.g., 2.31–2.35 Å in $K_3Zr_6Cl_{15}Be$ where the cluster also has $\bar{1}$ symmetry.[15] The Zr–$Cl^i$ distances average 2.57 Å, the Zr–$Cl^a$ distances are somewhat longer, 2.667 (3) Å, and the Zr–$Cl^{a-a}$ distances are longer yet, 2.772 (3) Å, as expected. Interestingly,

**Table IV.** Positional Parameters for $Cs_3Zr_6Cl_{16}C$

| atom | x | y | z |
|---|---|---|---|
| Zr(1) | 0.1151 (2) | 0.0928 (2) | 0.9049 (1) |
| Zr(2) | 0.8233 (2) | 0.0965 (2) | 0.9032 (1) |
| Zr(3) | 0.0488 (2) | 0.1359 (2) | 0.1323 (2) |
| Cl(1) | 0.6053 (5) | 0.2044 (4) | 0.7925 (4) |
| Cl(2) | 0.8557 (5) | 0.2619 (5) | 0.0391 (4) |
| Cl(3) | 0.1781 (5) | 0.2588 (5) | 0.0402 (4) |
| Cl(4) | 0.0712 (5) | 0.7909 (5) | 0.2154 (4) |
| Cl(5) | 0.7425 (5) | 0.3002 (5) | 0.2930 (5) |
| Cl(6) | 0.1695 (4) | 0.4955 (5) | 0.4970 (4) |
| Cl(7) | 0.2472 (5) | 0.5427 (4) | 0.2401 (4) |
| Cl(8) | 0.5752 (5) | 0.5509 (4) | 0.2469 (4) |
| Cs(1)[a] | 0.6045 (2) | 0.0285 (2) | 0.2878 (2) |
| Cs(2)[b] | 0.5100 (3) | 0.2969 (3) | 0.0218 (3) |
| C[c] | 0 | 0 | 0 |

[a] Occupancy refined to 0.983 (7). [b] Occupancy refined to 0.535 (6). [c] Occupancy refined to 1.2 (1).

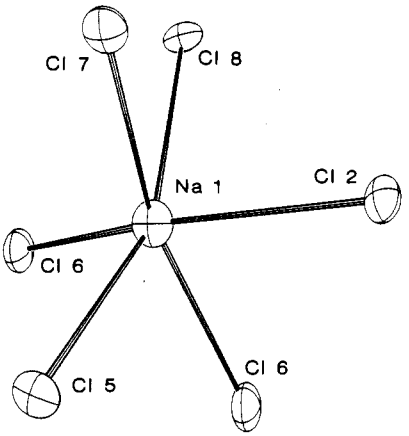


**Figure 2.** Chlorine environment around the Na(1) site within the layers in $Na_4Zr_6Cl_{16}Be$. The two shortest Na(1)–Cl distances are to the unshared terminal Cl(6) atoms. All ellipsoids are drawn at a 50% probability level.

the Zr(1)–Cl(7)$^{a\text{-}a}$–Zr(2) intercluster bridge has the longest Zr–Cl$^{a\text{-}a}$ distances observed to date in any of the zirconium chloride cluster phases, and the bridge is bent at the atypical angle of 161°, about midway between the more commonly observed angles of ~140 and 180°.[7,14,15,18] These parameters appear to reflect distortions in the layers that are necessary to accommodate the cations.

The sodium atoms occupy three distinct crystallographic sites that are defined either by the packing of the layers or by the matrix provided within the layer itself. Partial occupancy of two of the former sites coupled with the complete occupation of the third site within the layers gives a refined composition of $Na_{3,9(1)}Zr_6Cl_{16}Be$. Complete occupation of all of the sodium sites would give a total of five cations per cluster and a 15-electron cluster with beryllium within.

The Na(1) atom occurs in a fully occupied, six-coordinate site situated between clusters and *within* the cluster layer. The site deviates ±0.7 Å from the [100] plane about which the layer is centered and is about the same level as the Cl$^{a\text{-}a}$ atoms within that layer. The chlorine polyhedron about Na(1) shown in Figure 2 can be viewed as a highly distorted octahedron with Na–Cl distances ranging from 2.68 to 3.06 Å.

A Na(2) site that is only ~60% occupied lies ~1.7 Å above and below the same cluster layers and at about the same level as the Cl$^a$ atoms from the cluster layers above and below (see Figure 1). Five chlorine atoms surround the site (Figure 3) at distances of less than 3.00 Å, while a sixth chlorine atom, Cl(7)$^{a\text{-}a}$, is at 3.16 Å. The third sodium site, illustrated in Figure 4, lies on the 2-fold axis parallel to $\vec{c}$ in the tunnel-like structure between layers (Figure 1). The site is ~80% occupied and is surrounded by six chlorine atoms in a distorted trigonal antiprism at distances from 2.75 to 3.15 Å.

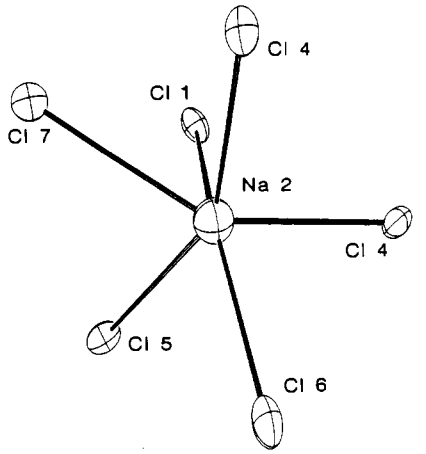


**Figure 3.** Six-coordinate Na(2) site between the layers in $Na_4Zr_6Cl_{16}Be$. The site has no crystallographically imposed symmetry (50% ellipsoids).

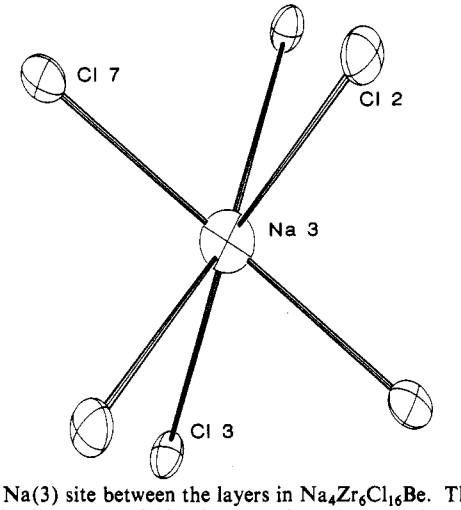


**Figure 4.** Na(3) site between the layers in $Na_4Zr_6Cl_{16}Be$. The six-coordinate site lies on a 2-fold axis approximately normal to the page. There are no terminal Cl(6)$^a$ within 4.0 Å. The shortest Na(3)–Cl distances are to Cl(7)$^{a\text{-}a}$ (50% ellipsoids).

The stoichiometry of the phase $Na_4Zr_6Cl_6Be$ is evidently largely controlled by the energetic advantages of achieving a 14-electron cluster,[7,13] even though this leaves the phase one sodium short of filling all cation sites fully. The distribution of sodium among the three cation sites appears to be controlled largely by electrostatic factors. The Na(2) site at 60% occupancy has two next-nearest zirconium neighbors at 3.8–3.9 Å. The Na(3) site, 80% occupied, has two zirconium neighbors at 3.95 Å, and the smallest and fully occupied Na(1) site has only one zirconium neighbor at 4.08 Å. A second sodium cation lies 3.72 Å from Na(1), but this should be electrostatically less important than the distances to the presumably more positively charged zirconium atoms. In addition, two short contacts of Na(1) with the more negative terminal Cl(6)$^a$ atoms in the structure make this site the preferred cation position.

**$Cs_3Zr_6Cl_{16}C$.** The structure of $Cs_3Zr_6Cl_{16}C$ (Figure 5) is clearly related to that of $Na_4Zr_6Cl_{16}Be$ and likewise contains stacked, two-dimensional sheets of $Zr_6Cl^i_{12}C$ clusters with the connectivity $^2_\infty[Zr_6Cl^i_{12}C]Cl^{a\text{-}a}{}_{4/2}Cl^a{}_2$. However, the need to accommodate the larger cesium cations results in some interesting modifications of the cluster layers and their stacking.

The cluster layers, which run in the 10$\bar{1}$ direction in $P2_1/n$, have a significantly more buckled appearance than those in $Na_4Zr_6Cl_{16}Be$, with the clusters now canted nearly ±30° from the normal to the cluster layers. The buckling also reduces the Zr–Cl$^{a\text{-}a}$–Zr intercluster bridging angle to a more typical value of 133°. The comparison with the $Na_4Zr_6Cl_{10}Be$ structure is made clearer by transformation of the present structure from $P2_1/n$ to $P2_1/c$, which places the cluster sheet in the [100] plane. This shows that although the repeat distance in the stacking direction is only one

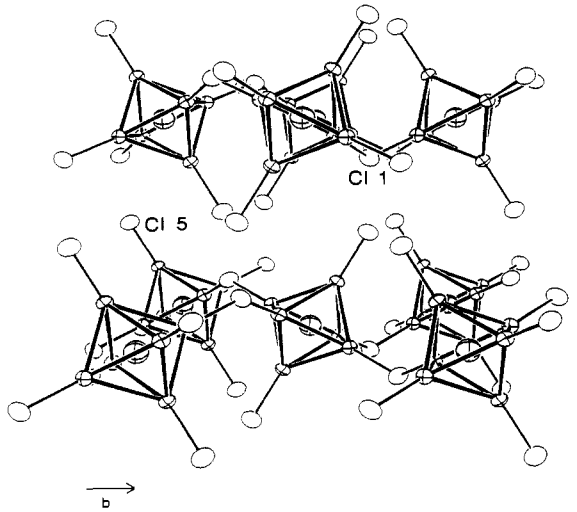


**Figure 5.** Approximately [001] view of the structure of $Cs_3Zr_6Cl_{16}C$. The $\vec{a}$ axis in the $P2_1/c$ setting runs from the closer lower left cluster to the upper left cluster. All $Cl^i$ and Cs atoms have been omitted for clarity (90% ellipsoids).

layer thick, the layers are stacked such that clusters in one layer lie over voids in the layers above and below, with the cluster layers related by screw axes between them. The translation of the cluster layers is described by the ~130° monoclinic angle. Conversion of the cell to one with pseudoorthorhombic symmetry with $Na_4Zr_6Cl_{16}Be$-type geometry (Figure 1) reveals that the 90° angle between the cluster layers and the stacking direction has now opened up to 97.4°. The interlayer distance, 9.44 Å, has also increased in order to accommodate the larger cesium cations. The small tunnel-like structures between layers in $Na_4Zr_6Cl_{16}Be$ have also disappeared as a consequence of the increased tilt of the clusters.

The $Zr_6Cl_{12}C$ cluster in $Cs_{3.0}Zr_6Cl_{16}C$ is only the second 15-electron cluster prepared in the zirconium chloride system, the other being $KZr_6Cl_{15}N$,[15] and the first for which we have detailed structural data. According to the interatomic distances compiled in Table V, the present phase exhibits Zr–C and Zr–Zr distances that are consistently shorter than those in the corresponding 14-electron, carbon-centered clusters. The Zr–C distances average 2.261 Å, which gives an effective carbon crystal radius of 1.40 Å, a value identical with that seen in the 16-electron cluster $Zr_6I_{12}C$[13] and shorter than the 1.42–1.43-Å distance in most 14-electron examples.[23] The Zr–Zr distances average 3.197 Å, about 0.025 Å less than the average Zr–Zr distances in the 14-electron clusters $KZr_6Cl_{15}C$[15] and $Na_{0.5}Zr_6Cl_{15}C$.[18] The Zr–Cl distances are slightly shorter than those in $Na_4Zr_6Cl_{16}Be$, but follow the same trend. The Zr–$Cl^a$ distance is 2.596 (6) Å and the Zr–$Cl^{a-a}$ distances average 2.689 Å.

The $Cs_3Zr_6Cl_{16}C$ structure has two distinct crystallographic cation sites that are virtually identical in geometry and capable together of accommodating up to four cations per cluster. The sites available between the layers in this phase for the larger cesium are of lower symmetry, somewhat reminiscent of the cation sites occupied in the three-dimensional cluster network in $CsKZr_6Cl_{15}B$.[14]

The fully occupied Cs(1) sites lie approximately one-third and two-thirds of the way between cluster layers, associated with voids in the cluster layer closest to them. This somewhat oversized site, shown in Figure 6, has no crystallographically imposed symmetry and is surrounded by seven chlorine atoms at an average distance of 3.645 Å, compared with a crystal radius sum of 3.55 Å for CN = 8.[24] Six chlorine atoms form a ring slightly below the cation, while the seventh Cl(2) atom lies above and over an edge of the ring. Three additional chlorine atoms between 3.90 and 3.92 Å away fill out the coordination sphere above and below the ring.

(23) Ziebarth, R. P.; Corbett, J. D. *J. Am. Chem. Soc.*, in press.
(24) Shannon, R. D. *Acta Crystallogr., Sec. A* **1976**, *A32*, 751.

**Table V.** Interatomic Distances in $Cs_3Zr_6Cl_{16}C$ (Å)

| | | | |
|---|---|---|---|
| | | Zr–Zr | |
| Zr(1)–Zr(2) (×2)[a] | 3.197 (3) | Zr(2)–Zr(3) (×2) | 3.188 (3) |
| Zr(1)–Zr(2) (×2) | 3.214 (3) | Zr(2)–Zr(3) (×2) | 3.190 (3) |
| Zr(1)–Zr(3) (×2) | 3.182 (3) | $\bar{d}$ | 3.197 |
| Zr(1)–Zr(3) (×2) | 3.212 (3) | | |
| | | Zr–C | |
| Zr(1)–C (×2) | 2.272 (2) | Zr(3)–C (×2) | 2.249 (2) |
| Zr(2)–C (×2) | 2.261 (2) | $\bar{d}$ | 2.261 |
| | | Zr–$Cl^i$ | |
| Zr(1)–Cl(8) (×2) | 2.537 (5) | Zr(2)–Cl(6) (×2) | 2.582 (5) |
| Zr(1)–Cl(4) (×2) | 2.544 (5) | Zr(3)–Cl(8) (×2) | 2.536 (5) |
| Zr(1)–Cl(3) (×2) | 2.545 (6) | Zr(3)–Cl(3) (×2) | 2.547 (6) |
| Zr(1)–Cl(6) (×2) | 2.583 (5) | Zr(3)–Cl(2) (×2) | 2.566 (6) |
| Zr(2)–Cl(4) (×2) | 2.528 (5) | Zr(3)–Cl(7) (×2) | 2.570 (5) |
| Zr(2)–Cl(2) (×2) | 2.543 (6) | $\bar{d}$ | 2.553 |
| Zr(2)–Cl(7) (×2) | 2.552 (5) | | |
| | | Zr–$Cl^{a-a}$ | |
| Zr(2)–Cl(1) (×2) | 2.697 (5) | Zr(3)–Cl(1) (×2) | 2.682 (6) |
| | | Zr–$Cl^a$ | |
| Zr(1)–Cl(5) (×2) | 2.596 (6) | | |
| | | Cs–Cl | |
| Cs(1)–Cl(5) (×1) | 3.498 (6) | Cs(2)–Cl(1) (×1) | 3.514 (6) |
| Cs(1)–Cl(1) (×1) | 3.542 (6) | Cs(2)–Cl(5) (×1) | 3.558 (6) |
| Cs(1)–Cl(5) (×1) | 3.554 (6) | Cs(2)–Cl(5) (×1) | 3.602 (6) |
| Cs(1)–Cl(4) (×1) | 3.658 (6) | Cs(2)–Cl(4) (×1) | 3.656 (6) |
| Cs(1)–Cl(8) (×1) | 3.700 (5) | Cs(2)–Cl(8) (×1) | 3.664 (6) |
| Cs(1)–Cl(2) (×1) | 3.775 (6) | Cs(2)–Cl(3) (×1) | 3.766 (6) |
| Cs(1)–Cl(7) (×1) | 3.791 (5) | Cs(2)–Cl(2) (×1) | 3.776 (6) |
| Cs(1)–Cl(6) (×1) | 3.908 (6) | Cs(2)–Cl(6) (×1) | 3.942 (6) |
| Cs(1)–Cl(3) (×1) | 3.917 (6) | Cs(2)–Cl(8) (×1) | 4.027 (6) |
| Cs(1)–Cl(6) (×1) | 3.919 (6) | Cs(2)–Cl(6) (×1) | 4.055 (6) |
| $\bar{d}$ | 3.726 | $\bar{d}$ | 3.756 |

[a] Number of times the distance occurs per cluster or cation.

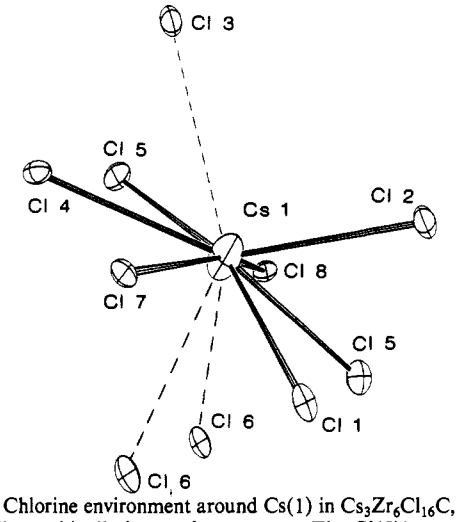


**Figure 6.** Chlorine environment around Cs(1) in $Cs_3Zr_6Cl_{16}C$, which has no crystallographically imposed symmetry. The Cl(5)[a] atoms are unshared terminal chlorine atoms. The dashed lines represent distances over 3.90 Å (50% ellipsoids).

Dashed lines have been included for the three greater separations in Figure 6.

The second cesium site, pictured in Figure 7, is nearly identical in size and shape with the Cs(1) site just described. Topologically, the site is composed of 10 chlorine atoms, two above a six-membered ring and two below. The cesium atom sits slightly above the six-membered ring. As in Figure 6, the dashed Cl–Cs(2) separations are approximately 0.2 Å longer than any of the others. The Cs(2) site is situated approximately midway between cluster layers and has a refined occupancy of 0.535 (6) Å, giving a phase composition $Cs_{3.0}Zr_6Cl_{16}C$. The site is just 0.03 Å larger than the Cs(1) site in terms of the seven-neighbor average, and this would appear to account for its partial occupancy compared with

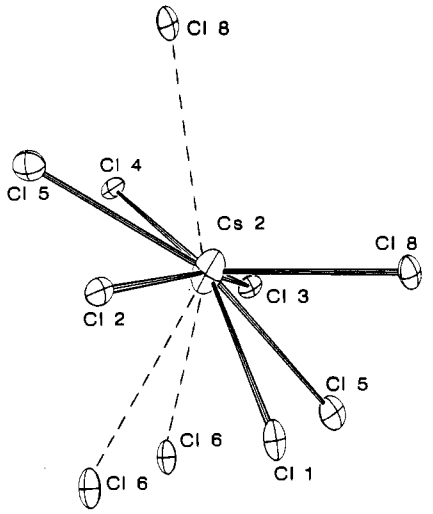


**Figure 7.** Cs(2) site in $Cs_3Zr_6Cl_{16}C$, which shows a remarkable similarity to the Cs(1) site (Figure 6). Dashed lines indicate distances over 3.90 Å (50% ellipsoids).

the full occupancy of the smaller Cs(1) site. The phase is probably nonstoichiometric in this respect. Changing the interstitial to beryllium presumably provides a full occupancy of cation sites in the phase $Cs_4Zr_6Cl_{16}Be$ that was also synthesized.

Surprisingly, the rather unusual chlorine environment around both of the cesium atoms appears to affect their thermal parameters only slightly, such that both are somewhat elongated in the direction perpendicular to the "$Cl_6$ ring" (~2:1) (compare $CsKZr_6Cl_{15}B$[14]).

The $Cs_3Zr_6Cl_{16}C$ structure and hence that of $Na_4Zr_6Cl_{16}Be$ show an unmistakable similarity to the structure of $K_3Zr_6Cl_{15}Be$.[15] The puckered square netlike sheets of $Zr_6Cl_{12}Z$ clusters found in the last beryllide are clearly evident lying perpendicular to $\vec{a}$ in Figure 7 in ref 15. The linear $Cl^{a-a}$ bridges that link these layers in $\vec{a}$ have disappeared in $Cs_3Zr_6Cl_{16}C$ as a result of the addition of another chlorine atom to each cluster. The cluster layers in the new cesium phase have also been translated half a unit cell in the $\vec{b}$ and $\vec{c}$ directions with respect to one another to make room for the additional chlorine atoms and have opened up slightly, reducing the cluster tilt. The $(\vec{b} + \vec{c})/2$ translation of the cluster layers with respect to one another may also be thought of as a reflection of every other layer through a mirror plane lying in the cluster layer. The end result in either case is the same; i.e., every cluster layer is puckered in the same direction at the same time. The relationship between the cation sites in the two structure types is considerably less clear because of the layer translation.

The layerlike structures of $Na_4Zr_6Cl_{16}Be$ and $Cs_3Zr_6Cl_{16}C$ offer an opportunity to pursue an intercalation/ion-exchange chemistry similar to that of the more common layered $MX_2$ compounds.[25] The flexibility of the cluster sheets that can be achieved through rotation and bending of the $Zr-Cl^{a-a}-Zr$ bonds should allow many differently sized and shaped monoatomic and polyatomic cations to be accommodated. Oxidation or reduction of the $Zr_6Cl_{12}Z$ clusters under mild conditions may also be possible. Two exploratory ion-exchange reactions of $Na_4Zr_6Cl_{16}Be$ with $KAlCl_4$ and $CsAlCl_4$ at 300 and 400 °C, respectively, appear encouraging in that reactions occurred in both cases judging from powder patterns of the products. Unfortunately, the flexibility of cluster sheets that makes them attractive host materials also makes indexing and interpretation of the powder diffraction patterns difficult because of the large intensity and line position changes associated with the puckering of the cluster sheets. Thus far, neither ion-exchange product has been characterized further.

The phase $Na_4Zr_6Cl_{16}Be$ also shows hints of what may be an interesting solution chemistry. It dissolves in acetone to give a dark red-violet solution that becomes colorless in air within minutes with the formation of a white precipitate. Further study will be required to determine if the chemistry can be controlled or is of interest.

**Acknowledgment.** We are indebted to Professor R. A. Jacobson for the continued provision of diffraction and computing facilities. This research was supported by the National Science Foundation, Solid State Chemistry, via Grant DMR-8318616, and was carried out in facilities of Ames Laboratory, DOE. R.P.Z. was also the holder of Departmental Gilman and Procter and Gamble Fellowships.

**Supplementary Material Available:** Tables of anisotropic thermal parameters for $Na_4Zr_6Cl_{16}Be$ and $Cs_3Zr_6Cl_{16}C$ and crystallographic details (3 pages); a listing of the observed and calculated structure factor data for the same compounds (12 pages). Ordering information is given on any current masthead page.

(25) Rouxel, J. *Intercalated Layered Materials*; Levy, F., Ed.; D. Riedel Publishing Co.: Dordrecht, The Netherlands, 1979; pp 201-250.

Contribution from the Departments of Chemistry, Iowa State University, Ames, Iowa 50011, and Texas A&M University, College Station, Texas 77843

# Encapsulation of Heavy Transition Metals in Iodide Clusters. Synthesis, Structure, and Bonding of the Unusual Cluster Phase $Y_6I_{10}Ru$

Timothy Hughbanks[1a] and John D. Corbett*,[1b]

*Received August 19, 1988*

The reaction of $Y_3Ru$ with $YI_3$ at 800-950 °C in a sealed Ta container affords $Y_7I_{12}Ru$ and $Y_6I_{10}Ru$, the yield of the latter increasing with time or temperature. $Y_7I_{12}Ru$ is isostructural with $Sc_7Cl_{12}B$ on the basis of Guinier powder data ($R\bar{3}$, $Z = 3$, $a = 15.4373$ (7) Å, $c = 10.6126$ (6) Å). The new structure type of $Y_6I_{10}Ru$ was deduced from its lattice dimensions and symmetry and was refined with single-crystal X-ray diffraction data ($P\bar{1}$, $Z = 1$; $a = 9.456$ (2) Å, $b = 9.643$ (2) Å, $c = 7.629$ (1) Å, $\alpha = 97.20$ (2)°, $\beta = 105.04$ (2)°, $\gamma = 107.79$ (2)°; $R = 5.2$, $R_w = 6.7\%$ for 1421 independent reflections, $2\theta \leq 55°$, Mo K$\alpha$ radiation). The structure consists of $Y_6I_{12}$ clusters centered by Ru and condensed into infinite chains through sharing of inner iodine ($I^i$) atoms with the two adjoining clusters, viz., $Y_6I^i_8I^{i-i}_{4/2}Ru$. The clusters are connected in the other two directions through the more typical $I^{i-a}$ linkages at metal vertices. The nominal octahedral $Y_6Ru$ cluster shows a 0.21-Å tetragonal *compression*, contrary to the usual behavior of $ML_6$ units with a $t_{1u}^4$ HOMO. Charge-iterative extended Hückel calculations show that the distortion originates with Y-Y interactions because of a negligible participation of the high-lying Ru 5p orbitals in the HOMO.

## Introduction

A remarkable feature of metal halide clusters composed of the electron-poorer transition metals such as zirconium and the rare-earth elements is that all $M_6X_{12}$-type clusters appear to *require* an interstitial heteroatom Z within. The interstitial atom in this role provides both additional bonding electrons and orbitals for the formation of strong M-Z bonds within the cluster. Although zirconium chloride clusters are the more versatile struc-

(1) (a) Texas A&M University. (b) Iowa State University.

0020-1669/89/1328-0631$01.50/0 